SYNTHESIS AND CHARACTERISATION OF NANO-AL_2O_3 REINFORCED AA6061

M. Hüller, J. Vlcek
EADS Corporate Research Centre Germany, P.O.B. 800465, 81663 Munich, Germany

Keywords: *Milling, Metal Matrix Composite, AA6061, Nano-particle, Calorimetry*

Abstract

AA6061 aluminium alloy powder and nano-sized alumina powder were mechanically alloyed by means of ball milling, followed by hot isostatic pressing and extrusion. Investigations of the microstructure revealed uniform dispersion of the reinforcements to an agglomeration size smaller than 800 nm. Mechanical properties were determined by static tensile tests. The influence of the mechanical activation and the nano-sized reinforcements upon the aging characteristics was investigated by DSC.

1 Introduction

Metal Matrix Composites (MMCs) combine a high strength and a high modulus. Therefore Al-Mg-Si alloys reinforced with alumina particles are being employed in automotive and aerospace applications today. With respect to the mechanical properties, the main drawback of these materials is their low ductility as the ceramic reinforcements promote the nucleation, growth, and coalescence of voids. With decreasing size of micro scaled reinforcements the strength tends to increase [1]. It is the reason why the incorporation of nanometric particles has received considerable attention. Their small size (<100 nm) can lead to an improved mechanical performance of metal matrix composites [2].
Concerning the processing of MMCs many techniques have been explored to synthesize metal matrix composites. Liquid phase processes often showed bad wetting of the reinforcements especially for nano-particles, which lowers the strength properties. This is mainly due to the high surface area and the strong agglomeration tendencies [3]. To avoid this problem and to support the dispersion of the nano-metric reinforcements a solid phase method is used for the processing here.
This paper studies the dispersion of Al_2O_3 nano-particle in the AA6061 matrix. The mechanical properties of the MMC were evaluated by static tensile tests in the consolidated condition. Differential scanning calorimetry (DSC) was carried out to look into the changed precipitation sequence. This was indicated by a lack of hardness.

2 Experimental Procedures

Argon-atomized AA6061 powder with an average particle size of 60 µm was used as the matrix. Nano-sized Al_2O_3 powder, synthesized by hydrothermal processing, with a mean size of 80 nm and an agglomeration size of 2 - 6 µm was adopted as the reinforcement (Fig. 1).

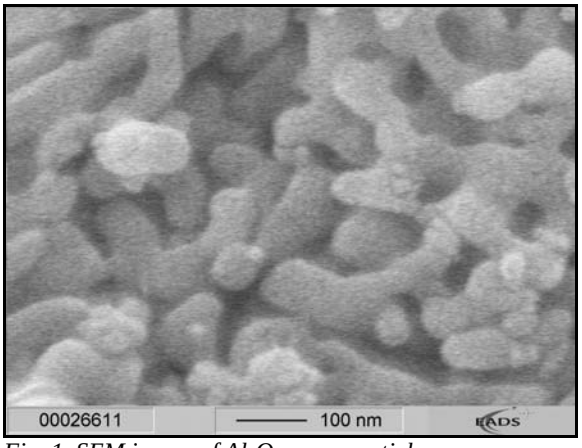

Fig. 1. SEM image of Al_2O_3 nano-particles

The powders were mechanically alloyed using a Fritsch “pulverisette 6” planetary ball mill with hardened steel balls and container. Milling was accomplished in an Argon filled glove box with a ball to powder weight ratio of 10:1. A MMC powder with 5 vol. % Al_2O_3 particulate reinforcement was fabricated. The distribution of the Al_2O_3 nano-particles inside the AA6061 matrix was investigated by scanning electron microscope (SEM) combined with focused ion beam (FIB) technique and Auger analysis.

After degassing the nano-particle reinforced powder was consolidated by hot isostatic pressing (HIP). Subsequently the extrusion with an extrusion ratio of 4:1 was carried out. The microstructure was investigated in the as-ground and the consolidated state. Static tensile tests of cylindrical test pieces and hardness tests were carried out in order to determine the mechanical properties.

The effect of mechanical activation upon the mechanical properties was investigated by calorimetry.

3 Results and Discussion

3.1 Microstructure

The optical micrographs of nano-reinforced MMC particles produced under different milling durations show the micro-structural evolution during milling (Fig. 2 and 3). Areas with high reinforcement content appear darkly. The images reveal that a prolonged milling time improves the dispersion of the second phase in the matrix. This is in accordance with the findings about mechanical alloying of ductile-brittle components [4]. In detail, the brittle particles tend to become occluded by the ductile constituents and incorporated in the ductile particles. The brittle constituent is closely spaced along the inter-lamellar spacing and gets uniformly dispersed as the lamellar get further refined. Nevertheless, after 8 h milling a lamellar structure is still visible (Fig 3).

In order to gain insight in the MMC and to visualize the nano-sized Al_2O_3 particles appropriate characterisation techniques had to be applied. The nano-particles were not well bonded to the matrix after the milling process. Thus metallographic preparation combined with SEM did not provide a sufficient insight into the material as the nano-particles were covered or torn away during polishing.

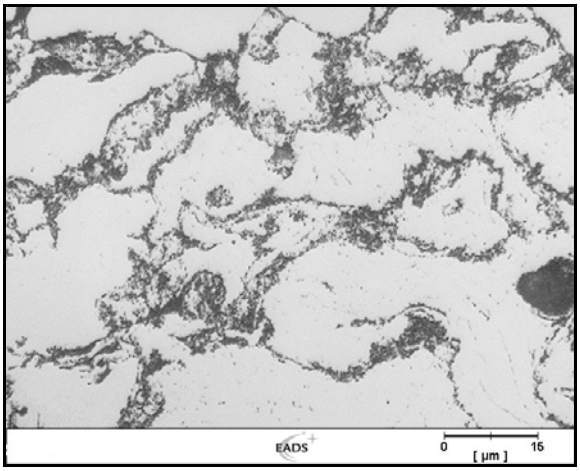

Fig. 2. Micrograph of AA6061/ nano-Al_2O_3 (5 vol. %) (milling time: 1h)

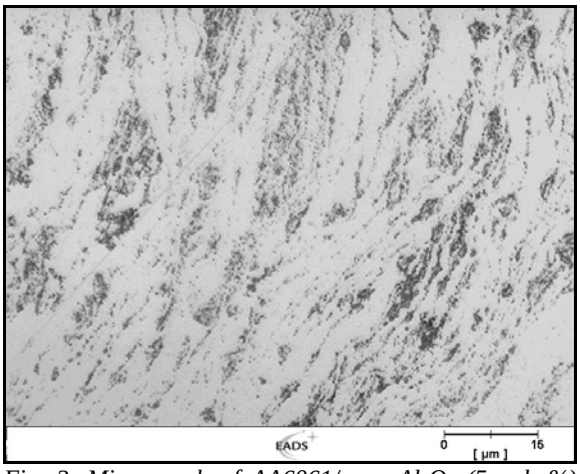

Fig. 3. Micrograph of AA6061/nano-Al_2O_3 (5 vol. %) (milling time: 8h)

SEM in combination with FIB depicted the microstructure of the MMC (Fig. 4). A notch with a depth of 20 µm was sputtered by means of Gallium ions into the surface of the micrograph. The plain perpendicular to the surface of the micrograph was investigated.

Nano-Al_2O_3 particle agglomerates were aligned partially agglomerated in layers (Fig. 5). This is the reason why the volume fraction of the second phase strongly depends on the investigated intersection. The surrounding of the

second phase particles indicated a weak particle/matrix interface. Numerous flaws were detected in these areas.

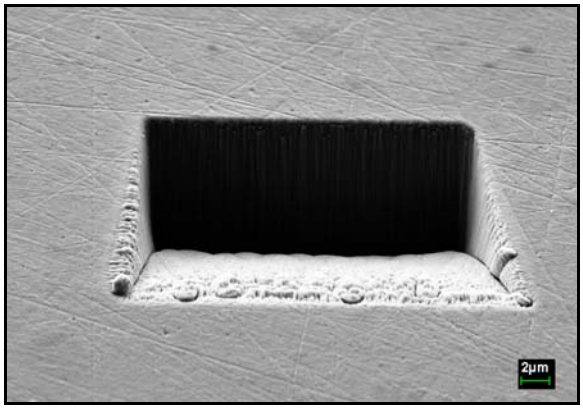

Fig. 4. Notch prepared by FIB in the cross section of a MMC powder particle

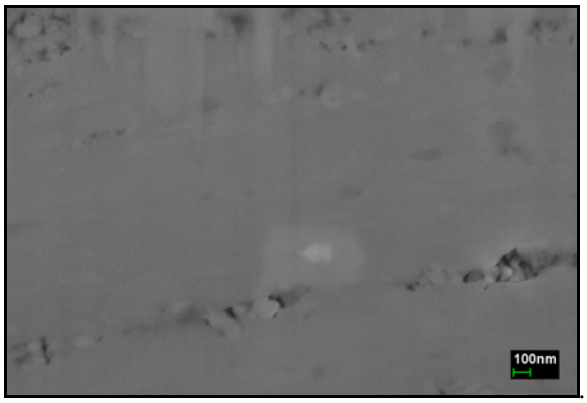

Fig. 5. Alignment of Al_2O_3 nano-particles in the AA6061 matrix

Additionally a qualitative determination of the Al_2O_3 particle distribution in the matrix was carried out by Auger analysis (Fig. 6). Before the characterisation 30 nm of the surface material was removed by Argon sputtering in order to exclude the influence of surface contamination and oxidation. The bright appearing sections refer to areas with high oxygen content and can be interpreted as a mapping of the Al_2O_3 particles. The results of the Auger analysis are consistent with the findings of the SEM/FIB investigation. It can be shown that the Al_2O_3 nano-particles were aligned in a lamellar structure in the AA6061 matrix after a milling time of 8 h. The spacing of the lamellae is in the range of 500 nm to 4 µm.

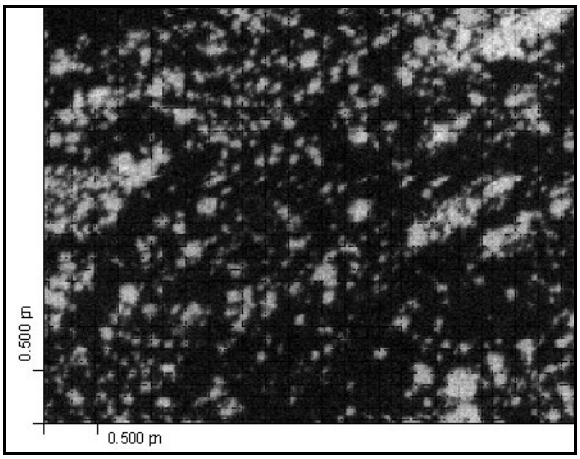

Fig 6. Oxygen map by means of Auger analysis depicts the Al_2O_3 distribution

After HIP the bonding of the second phase has been improved (Fig 7). Most of the nano-particles were not pulled out during polishing. Thus SEM investigation of micrograph is feasible in this condition. The flaws detected thereby were generated during metallographic preparation as some of the particles fell out. The lamellar structure produced in milling is still visible in this condition. Subsequent extrusion improved the dispersion of the second phase furthermore.

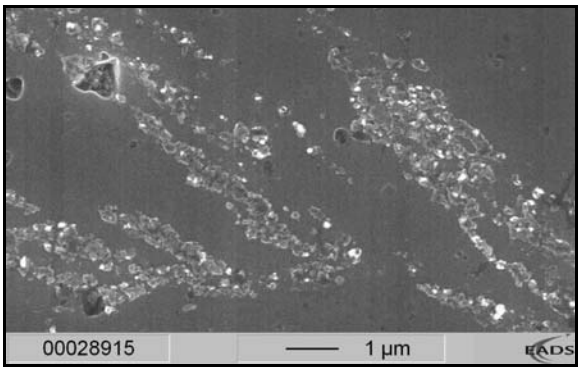

Fig. 7. SEM image of nano-particle reinforced AA6061 after HIP

3.2 Mechanical Properties

The mechanical properties of the MMC material were obtained by static tensile testing for two identical specimens in T6 condition

manufactured from HIP + extruded material (Fig. 8.). For comparison the values of standard AA6061-T6 material from literature are shown (Table 1).

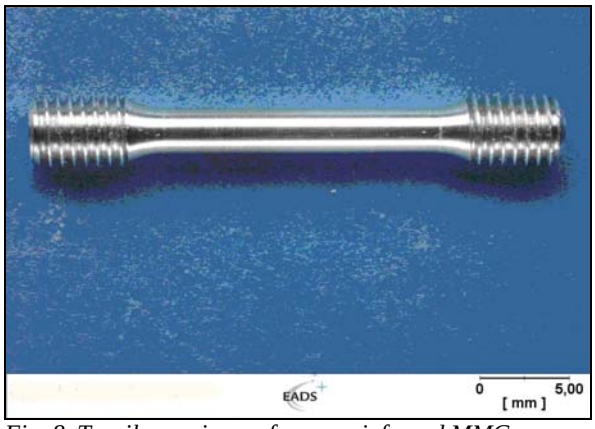

Fig. 8. Tensile specimen of nano-reinforced MMC

Table 1
Mechanical properties of the mechanical alloyed MMC specimens and AA6061 (literature) in T6 condition

Material	E [GPa]	Rp0,2 [MPa]	Rm [MPa]	A [%]
MMC	77,9	212	309	14
MMC	77,7	208	305	12
AA6061 [5]	69	280	310	12

The MMC specimens show an ultimate tensile strength which is comparable to the not reinforced AA6061 material. The yield strength is about 31% lower than that of the standard AA6061 material. The young's modulus for the reinforced specimens is 13% higher, which was expected from a law of mixture. It is surprising that the ductility of the nano-particle reinforced samples is as high as in the reinforced material. The ductile behaviour of the reinforced material is confirmed by analysis of the fracture surface (Fig. 9). A uniform structure of dimples with a size in the range of 1-3 µm was detected.
The high values for elongations of 12% and 14% respectively and the rather low strength properties indicate that the standard T6 precipitation hardening used for conventional AA6061 did not work for the AA6061 mechanical alloyed MMCs. It seems that after mechanical alloying the effect of precipitation hardening could not be used to full capacity. This would be in good accordance to the findings of Tatsuta et al. [6]. Tatsuta and his coworker report that mechanical alloying significantly reduced the age hardenability of P/M materials.

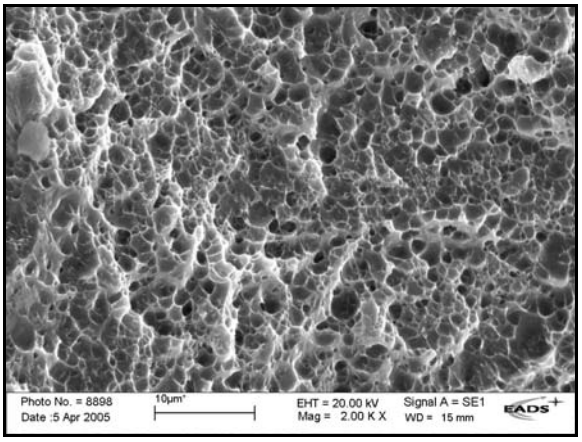

Fig. 9. SEM image of the fractured surface of the tensile specimen

This assumption was confirmed by hardness measurements of the MMC in the as-mechanically alloyed, hipped and hipped + aged condition (Table 2). The hardness of the as-mechanically alloyed condition is nearly twice as high as that in the hipped conditions. This is due to the cold working and the generated nano-sized grain structure. During solution annealing and precipitation hardening thermally activated processes lower the dislocation density and promote grain growth. This micro-structural evolution led to a strong decrease in hardness. The T6 heat treatment increased the hardness in the hipped condition only slightly, up to 3.8 % (Fig 9).

Table. 2. Hardness evolution after different processing steps

Condition	*As-ground*	*As-hipped*	*Hipped and T6 heat treated*
Hardness [HV1]	*176*	*88*	*91*

3.3 Precipitation sequence of mechanically alloyed AA6061

In order to interpret the mechanical properties especially the rather low values for yield

strength and ultimate tensile strength in the T6 condition it is necessary to investigate the precipitation sequence of mechanically alloyed AA6061.
The precipitation sequence of standard AA6061 is well investigated and was proposed to follow the steps [7]:

Clusters of Si atoms → GP-I zones → GPII-zones/β´´ → β´ → βMg_2Si

Fig. 10 depicts the corresponding DSC plots for AA6061 for different pre-aging states [8]. The exothermic reactions are plotted downwards. The peak at a temperature of about 249°C (522K) belongs to the precipitation of the GPII zone. The particles which precipitated during this reaction are responsible for the hardening effect in the T6 condition of AA6061. This peak was confirmed by DSC investigation of the AA6061 powder in the as-atomized condition.

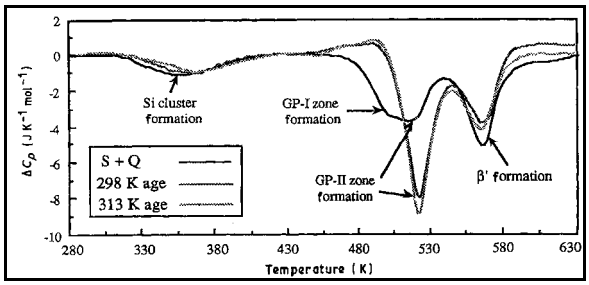

Fig. 10. DSC thermogram of the effect of pre-aging of AA6061 [8]

The DSC plot of the mechanically alloyed system in the as-mechanically alloyed state shows a much broader peak. This GPII peak is also shifted towards lower temperature at about 25°C. Here, the exothermic reaction is plotted upwards (Fig. 11).
The changed age hardening response of Al-Mg-Si alloys has been investigated by numerous studies before. Reasons for this behaviour are given in the following.
It has been shown by Rack [9] that the aging sequence is sensible to prior strain. During milling a high dislocation density is generated due to severe plastic deformation. These dislocations and the lattice distortion along the particle-matrix interface act as nucleation agents for the precipitates. Dislocations were also generated due to thermal mismatch between reinforcements and the matrix. Therefore the nucleation process is accelerated and early growth stages of the semi-coherent intermediate phase precipitations occur. This may yield an over-aged microstructure during aging at standard T6 parameters [10, 11, 12].

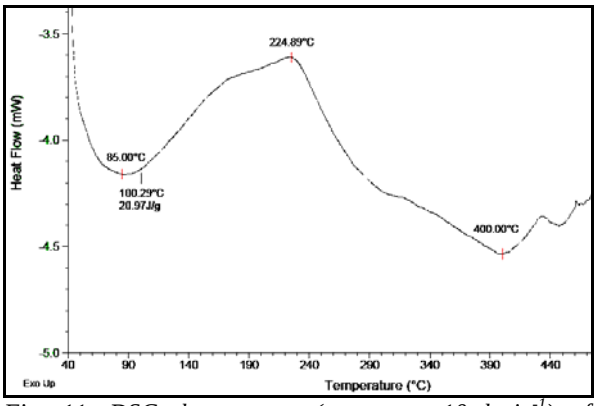

Fig. 11. DSC thermogram (scan rate 10 $kmin^{-1}$) of solutionized and quenched AA6061

In order to find out if a reduction of the ageing temperature leads to higher hardness the following investigations were carried out. Specimens in the as-hipped condition were heat treated at 150°C and 140°C for up to 25 hours; the standard T6 heat treatment proposes 160°C. The results show that except for a small hardness increase at 150°C for 3 h no increase hardness could be achieved (Fig. 12).

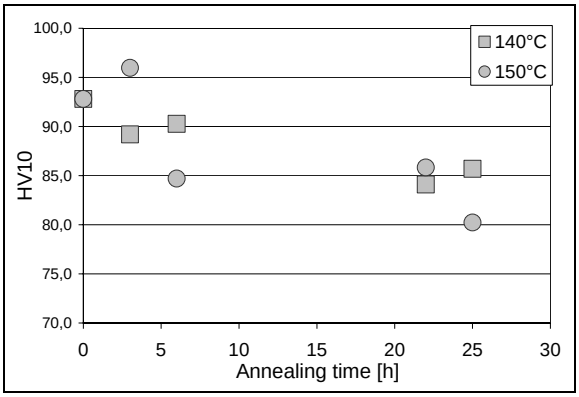

Fig. 12. Age-hardening curves after ageing at 140°C and 150°C

The results indicate that the precipitation sequence not only shifted towards lower

temperatures. It seems that a homogeneous precipitation of coherent and semi-coherent particles is not feasible in mechanical activated nano-particle reinforced material. Further investigations need to clarify if a heat treatment of several hours at a temperature in the range of the annealing temperature could diminish the effects of mechanical activation.

4. Conclusion

A MMC material based on Al_20_3 nano-particle reinforcements and AA6061 matrix was synthesized by powder metallurgy methods. The microstructure, mechanical properties and precipitation behaviour were investigated and compared with that of non-reinforced aluminium. The following conclusions are derived from the results:

1. Sub-micron scale clusters of Al_2O_3 particles were detected in the matrix after mechanical alloying. The reinforcements were located in a fine layered structure. According to SEM investigations the particle/matrix adhesion is rather weak in the as-ground condition but improved after hot isostatic pressing.
2. In comparison to the non-reinforced material the nano-MMC yielded the following mechanical properties: according to a rule of mixture the young's modulus was increased up to 13%.The yield strength is 31% lower and the ultimate tensile strength is about the same.
3. The precipitation sequence of mechanically alloyed powders revealed a shift of the GPII peak by 25°C to lower temperature in the DSC plot. The peak of the milled powder has also changed to a wider and less defined shape. It is assumed that the increased dislocation density and the high amount of interfaces and vacancies act as nucleation agents for the precipitates. Consequently an over-aged microstructure is obtained by standard T6 heat treatment which did not promote an increase in hardness.

Acknowledgments

This research was supported by the European Space Agency (N°17829/03/NL/SFe).

References

[1] Yang J; Cady C, Hu MS, Zok R. Effect of damage on the flow strength and ductility of a ductile Al alloy reinforced with SiC particulates. *Acta Metall Mater*, Vol. 38, pp 2613-2619, 1990.

[2] Ma ZY, Tjong SC, Li YL. The performance of aluminium-matrix composites with nanometric particulates Si-N-C reinforcement. *Composites Science and Technology*, Vol. 59, pp 263-270, 1999.

[3] Malchere A, Grosbras M, Demenet JL, Bresson L, Gaffet E. Study of an Al composite reinforced with nanometric SiC particles, produced by mechanical alloying, *Materials Science Forum*, Vol. 225-227, pp 763-768, 1996.

[4] Suryanarayana C: Mechanical alloying and milling. *Progress in Materials Science*, Vol. 46, pp 1-184, 2001.

[5] Brandes EA, Brook GB. Smithells Metals Reference Book. Seventh Edition, Butterworth Heinemann, 1999.

[6] Tatsuta, M, Kim, D-G; Kaneko, J; Sugamata, M.: Age hardening behavior of mechanically alloyed P/M aluminium alloys. The proceedings of International Conference on Recent Advances in Science and Engineering of Light Metals, Tokyo, *Science and Engineering of Light Metals*, 1991.

[7] Edwards GA. Stiller K, Dunlop GL, Couper MJ. The precipitation sequence in Al-Mg-Si alloys. *Acta mater.*, Vol. 46, No. 11, pp 3893-3904, 1998.

[8] Dutta I, Allen SM. *A calorimetric study of precipitation in commercial aluminium alloy 6061*, Journal of Materials Science Letters, Vol 10, pp 323-326, 1991.

[9] Rack HJ. The influence of prior strain upon precipitation in a high-purity 6061 aluminum alloy. *Materials Science and Engineering*, Vol. 29, pp 179-188, 1977.

[10] Lacom W, Spiradek K. Assessment of thermal-treatment conditions for age-hardenable particulate-reinforced aluminium alloys by calorimetric methods. *Thermochimica Acta*, Vol. 310, pp 125-132, 1998.

[11] Nieh TG, Karlak RF. Aging characteristics of B_4C-reinforced 6061-aluminum. *Scripta Metallurgica*, Vol. 18, pp 25-28, 1984.

[12] Seyed Reihani SM, Dafir D, Merle P. Experimental Analysis of the acceleration of β´precipitation in a 6061/SiCp composite; *Scripta Metallurgica et Materialia*, Vol. 28, pp 639-644, 1993.